Stick-slip dynamics of a one-dimensional array of particles

Farhang Radjai* and Pierre Evesque
Laboratoire de Mécanique des Sols, Structures et Matériaux, Ecole Centrale de Paris, Grande Voie des Vignes, 92295 Châtenay Malabry Cedex, France

Daniel Bideau
Groupe Matière Condensée et Matériaux, Université de Rennes 1, F-35042 Rennes Cedex, France

Stéphane Roux
Laboratoire de Physique et Mécanique des Milieux Hétérogènes, Ecole Supérieure de Physique et Chimie Industrielles de Paris, 10 rue Vauquelin, F-75231 Paris Cedex 05, France

(Received 5 April 1995)

The frictional motion of a linear array of parallel identical cylinders on a horizontal plane is studied both experimentally and analytically. An "irregular" stick-slip motion is observed in experiments. However, statistics on the forces before and after each slip show stable average behavior. We find that global dynamic and static coefficients of friction of the system increase with the number of particles. The organization of the rotations of particles appears as regions with characteristic lengths intermediate between the particle size and the size of the system. The mechanisms leading to these spatial patterns are studied analytically and are shown to be related to the interplay of the Coulombic friction law and the geometrical frustration of rotations. A simple argument based on the variation of the global friction force with the applied force on the array is proposed to account for the slip amplitude distributions observed in experiments.

PACS number(s): 46.10.+z, 46.30.Pa

I. INTRODUCTION

Granular media are dense disordered systems composed of particles with hard core interactions and frictional couplings. Macroscopically, quasistatic deformation of a granular system involves two basic features: (i) many metastable states and (ii) an instability threshold. In other words, the system stores potential energy up to a critical threshold and then releases part of it through dissipative fast events (avalanches, "plastic" flow). A general argument, issued from the concept of self-organized criticality [1], suggests that the distribution of these dissipative events should be generically large and span all length scales of the system. However, experiments on real sandpiles show that, although at the maximum angle of repose the distribution of avalanche sizes is large, "critical" fluctuations do not occur, so that a typical avalanche size can be defined [2,3]. On the other hand, earthquake models that combine a frictional threshold with elastic couplings between "blocks" seem to exhibit more naturally dissipative slipping events with power law distributions [4], although more recent investigations show that some characteristic event sizes emerge from the dynamics [5]. In these models, friction provides an instability threshold, which is fundamental to their chaotic nature. Friction in noncohesive granular systems plays an essentially different role in that it is *the* "contact law" between particles. Two particles may slide against each other, in which case the friction force at the contact point is fully mobilized, or they may simply roll one against another, in which case no dissipation takes place. Although rotations of particles provide a low-dissipative easy mechanism of deformation of a granular system, they are generally not sufficient to allow an arbitrary deformation to take place. Moreover, rotations of particles are frustrated as a result of geometrical disorder. Indeed, as soon as a "loop" of contacting particles contains an odd number of elements, rotations of the particles in the loop are not possible without friction being mobilized on at least one contact. Thus it is believed that dissipation is essentially due to dry interparticle and particle-boundary sliding friction [6]. In this way, nonlinear contact laws and geometrical disorder, as well as frustration of rotations, are pertinent components of granular systems, which limit the theoretical understanding in this domain [8].

In this investigation, we will consider a simple model that takes some of these aspects into account: an array of identical cylinders in mutual contact and supported by a plane. Since there is no interference with the effects of geometrical disorder, this model allows for a detailed study of the influence of friction on the organization of particle rotations in a context of complete frustration. This system can be viewed as the granular analog of a spring-block chain, with elastic contacts replaced by frictional rigid contacts and translational degrees of freedom turned into rotational ones. It incorporates frustration of

*Also at Groupe Matière Condensée et Matériaux, Université de Rennes 1, F-35042 Rennes Cedex, France.

rotations since a pair of two neigboring particles and the plane form a loop of three solids mutually in contact. We also remark that, although from the point of view of the centers of particles the model is "one dimensional," contact points are distributed in two rows. Hence the system can be considered as a medium composed of interparticle contacts and an interface with the plane through the particle-plane contacts.

A previous theoretical study of this model on the basis of Coulomb's law of friction has clarified the following points [7]. When pushed by a constant force in the direction of its mean orientation, the system evolves from a random distribution of initial angular velocities to a steady state, where the linear acceleration of the array and the angular accelerations of all particles remain constant in time. The steady state is independent of the initial state of velocities and involves a well-defined organization of rotations of particles and contact forces along the array. As a result, intermediate length scales appear in between the particle size and the size of the system. In this way, friction not only does not amplify disorder present in the initial state, but appears as an organizing agent driving deterministically the system to a stable steady state.

In this article, we present an experimental investigation of this system. The experimental setup and results are presented in Sec. II. In these experiments, the motion of the array and individual particles is intermittent: the particles stick to the plane while the driving force increases on the boundary, until the driving force becomes high enough to trigger a slipping motion of all particles. With a constant speed of the driving spring, the applied force is an "irregular" stick-slip signal. Statistics on the values of forces before and after each slip during an experimental run, as well as the rotations of particles, are on average well defined and show stable mean values. These results confirm again the idea that, even in the presence of noise, frictional couplings do not lead to a chaotic behavior. We will study, however, the sensitivity of the system to the boundary conditions and an amplification mechanism susceptible to enhance flutuations.

In Sec. III we will study the length scales appearing in the system, as well as the global coefficients of friction of the system as a single object in translation. We will present a steady-state approach, showing that in a noisy context the center of stick-slip oscillations is highly susceptible to fluctuations. A brief summary and some possible extensions of this investigation are presented in Sec. IV.

II. EXPERIMENTS

A. Experimental setup

The experimental setup is shown schematically in Fig. 1. Displacement of a long array of cylinders requires a long track and the driving device has to be parallel to the array in order to ensure translational invariance of the system. For this purpose, we have used a 3-m-long wooden table supported by three metallic bars fixed to a wall. It carries the pushing device and a long track A. In order to change the frictional properties of the track, the material the track is made of can be changed. The cylinders, all of the same size, are arranged on the track to form a chainlike system where each cylinder is in contact with its neighbors. The pushing device is a 60-kg metallic plate (the slider B) driven by a robust motor C and sliding with a constant speed on two parallel rails. A steel rod, fixed to the slider, carries at its other end a vertical brass beam D in direct contact with the array of particles. We used a complete Wheatstone bridge composed of four strain gauges as transducers. They were fixed on the beam in such way to compensate temperature gradients in the beam. The differential signal from the bridge was amplified, digitalized, and sent to a personal computer. In order to measure the rotations of the particles, experimental runs were filmed by a camera.

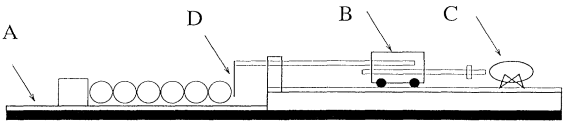

FIG. 1. Schematic view of the experimental setup (see the text).

Due to the sensitivity of granular media to boundary conditions, one important difficulty of these experiments is to keep the boundary conditions during an experimental run as invariable as possible. This demands a great stiffness of the pushing beam. On the other hand, the particles have a limited weight and the driving force is weak (smaller than $3N$ in our experiments). Hence the stiffness of the pushing beam should be small enough to allow for a reasonable signal-to-noise ratio. We have used a fix stiffness of $k = 10^4$ N/m, corresponding to a maximum relative deformation of 3×10^{-3} of the pushing beam. This is roughly the deviation from the vertical line and seems small enough for the driving force on the array to be considered as horizontal. Moreover, to improve the signal-to-noise ratio, we prepared special cylinders made of Plexiglas with brass cylindrical axis. This practically tripled the weight of cylinders. Since the particles rotate during the displacement of the array, the system cannot be translationally invariant if the particles do not have perfect circular sections. This was the main reason for choosing Plexiglas, which is generally protected by a plastic cover after fabrication. We also used polyvinyl dichloride (PVC) cylinders, which had a less regular surface. In all cases, the cylinders were cleaned with alcohol before each experiment.

Besides using stiff mechanical elements in the driving device in order to limit signal bias, we had also the freedom to choose a convenient rotation speed of the motor. The noise increased with the rotation speed, so that it was preferable to work at low speeds. On the other hand, a low speed implies a longer experiment with more external noise. We used an optimal translation speed of 21 μm/s. At this speed, a 1-h run delivered from 400 to 1200 stick-slip events depending on the number of particles. This corresponds in turn to a total displacement of 8 cm. A longer run increases the noise due to spatial

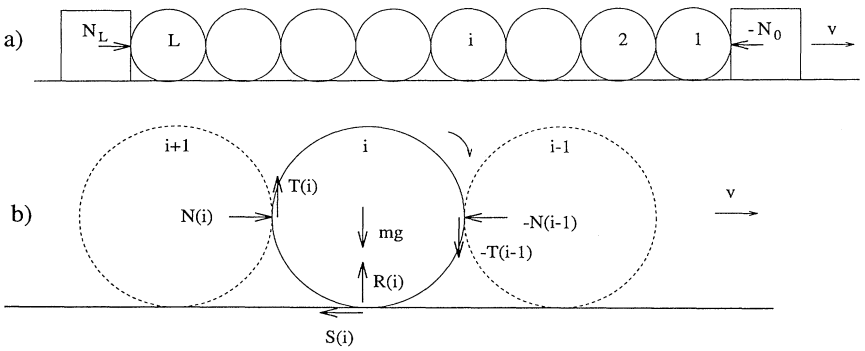

FIG. 2. (a) Representation of the array of particles. (b) Forces exerted on the particle i and sign conventions.

inhomogeneities of the track. Experiments on the spring-block system have shown that the setup parameters, such as speed and stiffness, have a determining effect on the dynamics [9,10]. Our investigations concern essentially the parameters relevant to the granular system, such as the number of particles and the coefficients of friction.

Figure 2 shows a schematic representation of the array with the sign conventions that will be used in Sec. III. In the first runs, we have used PVC cylinders of length 6 cm, diameter 2.5 cm, and an average weight 44 g. We used later also Plexiglas cylinders of length 4 cm, diameter 2 cm, and a weight of 56 g. Polystyrene, soft plastic, and wood were used for the track, but most of experiments were conducted with a polystyrene track. The static coefficients of friction of these materials are shown in Table I. These values have been obtained with our experimental setup from the motion of a block on a track. In order to avoid spontaneous rolling of the particles, which entails opening of interparticle contacts, we confine the array by a cubic block of small weight (a few grams) set in contact with the first particle of the array and moving with the array. As we shall see below, the confining charge is a useful control parameter when the driving force is weak. Although we have used different materials for the particles and the track, the study of the behavior of this system as a function of the coefficients of friction is only qualitative in these experiments. Hence the main parameters in our experiments are the number of particles L and the confining charge P.

B. Signal analysis

Figure 3 shows a typical example of the signal: the driving force oscillates between two levels. Each oscillation consists of a slow rising period and a short dropping period. During the rising period, the driving force increases linearly in time up to a maximum value. This corresponds to stick period, where the array is at rest and the pushing beam undergoes a constant-speed deformation. Hence the slope of the signal in the stick period is directly proportional to the pushing speed. The force needed to trigger sliding is the static friction force, which we will represent by F_s. The dropping period corresponds to a rapid sliding of the array down to a stop force N_f. A periodic stick-slip motion is characterized by giving only the two levels of slip and stop, and the pushing speed. Here, we have rather an "irregular" stick-slip motion with fluctuating levels. We tried to diminish these fluctuations by improving the experimental setup and the quality of the cylinders. These attempts not only did not diminish the fluctuations, but made them even more spectacular. This fact changed the scope of our study to extend it to statistics on the two levels and the difference between them, which is the force drop. We set up an algorithm to search for stick-slip events. The algorithm uses the derivative of the signal and a cutoff on slip amplitudes. Slips of an amplitude smaller than the noise level were rejected.

For a given set of parameters, we studied the stability in time and reproductibility of the system, which can only

TABLE I. Coefficients of static friction of the materials used in experiments.

Materials	Static coefficient of friction
PVC-PVC	0.23 ± 0.02
Plexiglas-Plexiglas	0.52 ± 0.13
PVC-polystyrene	0.44 ± 0.05
Plexiglas-polystyrene	0.52 ± 0.08
PVC-plastic	0.26 ± 0.02

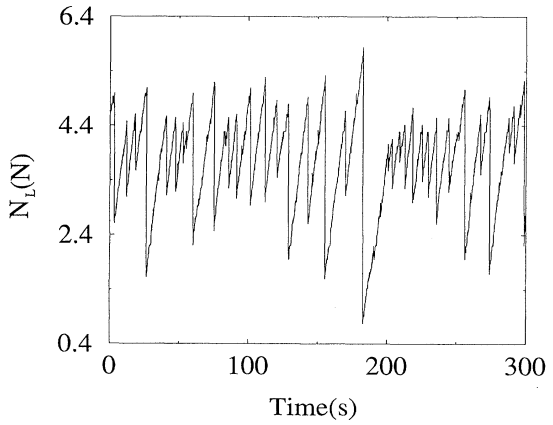

FIG. 3. Typical example of the stick-slip signal observed in experiments, corresponding to variations of the driving force N_L in time.

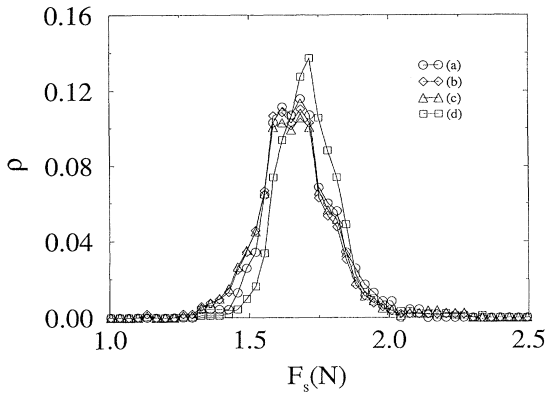

FIG. 4. (a), (b) and (c) Distributions for the slip force in three stages of an experiment with 15 particles. (d) Distribution for the slip force with the same system when the rotational degrees of freedom are blocked.

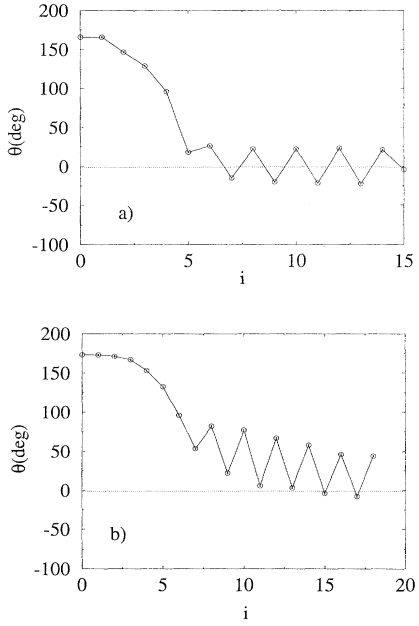

FIG. 5. Total rotations of particles during a 15-min experiment with (a) PVC particles on a soft plastic track and (b) Plexiglas particles on a polystyrene track. The rotation corresponding to the coordinate 0 stands for the total displacement of the array normalized with repect to the radius of one particle.

be defined statistically. Figure 4 shows the distributions for slip forces in three stages of an experimental run with 15 particles. These distributions are remarkably stable and reproducible. Thus the average quantities can be reproduced with a precision of the order of digitalization (a 12-bit analog-to-digital converter was used, which in association with the amplifier provided an absolute precision of $0.035N$). This stability also validates *a posteriori* the experimental setup.

C. Experimental results

We will study first the rotations of the particles. Since rotations are completely frustrated, dissipation at interparticle and particle-plane contacts is directly related to the rotations of particles. In this way, rotations provide a simple way to look into the spatial pattern of dissipation. Unless indicated otherwise, the experimental results presented here concern Plexiglas cylinders on a polystyrene track.

1. Rotation modes

Figure 5(a) shows the total rotations of the particles after a 15-min experimental run with PVC cylinders on a soft plastic track. We see that the organization of rotations appears as well-defined patterns. Three different behaviors appear successively along the array. One particle, the one in contact with the confining block, is just rolling without sliding on the plane. It has rotated by the same angle as the total displacement of the array, which is normalized with respect to the radius of one particle and shown at the coordinate zero. This mode of rotation will be referred to as phase 1. Then, we have four particles with rotation (in the positive direction) *and sliding* at the same time on the plane. In this phase, which will be referred to as phase 2, all of the contacts are sliding. Next, we have nine particles rotating in opposite directions and sliding on the plane. In this phase, which we will refer to as phase 3, all interparticle contacts are nonsliding. The particles in phases 1 and 2 are stable in time and the pattern is preserved. In phase 3, the pattern is preserved as well and there is a strong correlation of rotations along the array, but the direction of rotations is sometimes reversed or all particles in this phase may simply slide with no rotation. Experiments with Plexiglas cylinders on polystyrene track show the same three modes, as shown in Fig. 5(b). However, this pattern, in comparison to that of Fig. 5(a), is superposed by a constant rotation gradient. In Sec. III we will show that these patterns are directly related to Coulomb's friction law and variations of the applied force on the system during a slip.

2. Global coefficients of friction

Figure 4 shows that the distribution for slip force N_s is peaked on a mean value. This force at the threshold of slipping is equal to the friction force F_s of the whole system on the plane comprising the confining block. When normalized with respect to the total weight of the system, this mean value defines a "global coefficient of friction" M for the system in translation on the plane. The same figure shows also the distribution for slip force of the same system when the rotational degrees of freedom of the particles are blocked. In this case, the peak is narrower and centered on a larger force. This shift results obviously from the rolling of some particles. But a theoretical approach should explain the way rolling on the plane takes place while all rotations are frustrated.

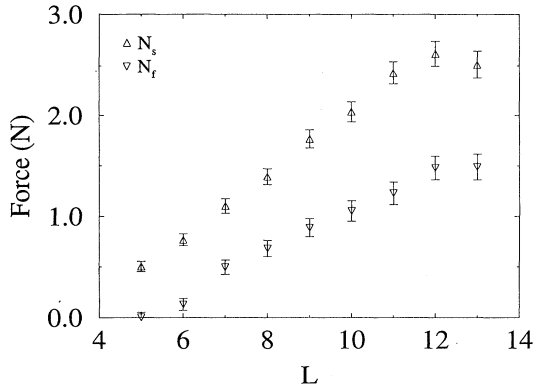

FIG. 6. Variation of the mean value of the slip force N_s and that of the stop force N_f as a function of the number of particles. The difference corresponds to the mean force drop.

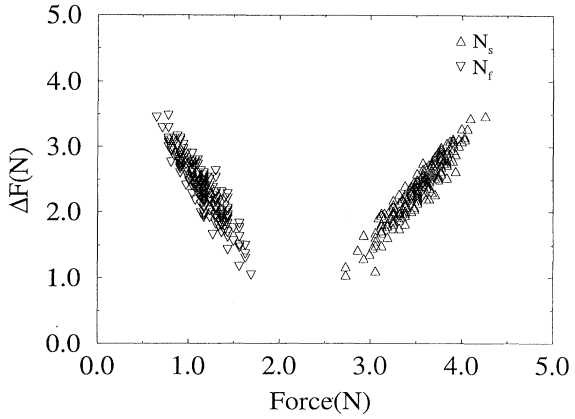

FIG. 8. Successive values of the force drop ΔF plotted as a function of the level N_s from which they start and the level N_f at which they stop during one experiment with an array of 12 particles.

In Fig. 6 the variation of the mean value of N_s and N_f is shown as a function of the number of particles. Each point corresponds to a 1-h experiment and several hundred stick-slip events. The coefficient of static friction is observed to increase linearly with the number of particles. When the latter is smaller than 6, all particles are in a rolling phase. As the number of particles increases, there are more and more particles in the second and then in the third phase. At the threshold of 12 particles, the last particle of the array rises up and loses its contact with the track. It is expected that as the number of particles in phase 3 increases, the friction should saturate to a value very close to the particle-plane coefficient of friction. It is not the case here because of the opening of the contact of the last particle with the plane. In all cases, the final coefficient of friction is always a little smaller than the plane-particle coefficient of friction since there are always particles in phase 1.

Figure 7 shows the variation of the static friction force N_s as a function of the weight P of the confining block in an array of 14 particles. The friction increases rapidly with P up to a value smaller than the equivalent friction for a block. Instability of the contact of the last particle with the plane, when P becomes of the order of $0.5N$, influences the geometry and hence the driving force is no longer controlled only by the friction on the plane. Note the high sensitivity of the system to the confining force, where a small variation of the latter results in large variations of the global friction force on the plane.

3. *Correlations*

Although the stick-slip signal in our experiments is quite irregular, larger slips are generally those that follow a high slip force, where the system has stored a larger amount of potential energy. In Fig. 8 successive values of the force drop ΔF during one experimental run are plotted as a function of the level from which they start. The data collapse on a straight line with a mean slope of $S_s = 1.6$ and fluctuate around it with a constant ampli-

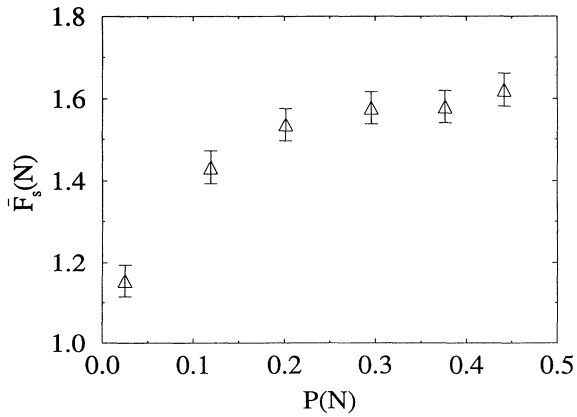

FIG. 7. Variation of the static friction force as a function of the weight P of the confining charge for an array of 14 particles.

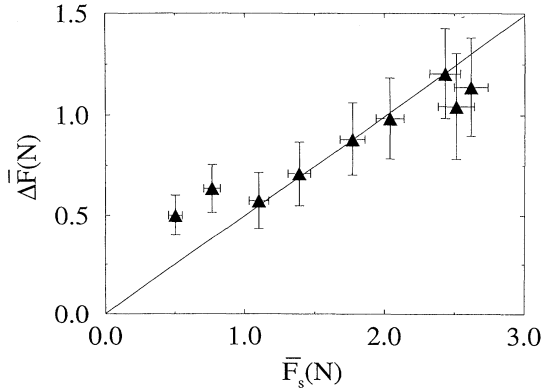

FIG. 9. Mean value of the slip force versus the mean value of the force drop for an increasing number of particles in the array. The leftmost point corresponds to an array of 5 particles and the rightmost point to an array of 13 particles.

tude. The slope is independent of the number of particles in the array. Also shown in the figure is the force drop as a function of the level at which it stops. This is again a straight line with a mean slope of $S_f = -2.6$. The two lines go through the same point F_d on the force axis where the force drop is zero. This point in the force space defines the center of stick-slip oscillations and corresponds to the dynamic coefficient of friction (Sec. III). So we have the empirical relation between the static friction force and the force drop

$$S_s = \frac{\Delta F}{F_s - F_d} = 1.6 \ . \tag{1}$$

It can also be seen from Fig. 8 that the highest value of the slip force is smaller than the value corresponding to the point $F_s = \Delta F$. In fact, the mean value of the slip force versus the mean value of the force drop defines a single point with coordinates $(\bar{F}_s, \Delta\bar{F})$. The diagram of these mean points when the number of particles changes is shown in Fig. 9. This is close to a linear relation. The intermediary part of the curve goes through the origin of axis and the slope is 0.5,

$$\frac{\Delta\bar{F}}{\bar{F}_s} = 0.5 \ . \tag{2}$$

For 12 particles the force drop is lower. This is due to the rising up of the last particle. For five and six particles the force drop is higher. In Sec. III we will see that this effect results from the variation of the center of oscillations. For an array of less than five particles we observe no stick-slip motion. From Eqs. (2) and (1) we get a relation between the mean values of static and dynamic friction forces for an array of Plexiglas particles on a polystyrene track, namely, $\bar{F}_d = 0.7\bar{F}_s$, which is independent of the number of particles.

Length scales appearing in the rotations of particles, the quasiperiodic nature of the stick-slip motion, the dissymmetry of this stick-slip motion with respect to the center of oscillations, and finally increasing the dynamic and static coefficients of friction in the same proportion with the number of particles are general features of the intermittent dynamics of an array of particles at least for the setup parameters of our experiments. Moreover, the dynamics is highly controlled by a small confining charge. In the following, we will discuss some of these aspects, which can be analyzed in the framework of a steady-state approach.

III. THEORY

The global behavior of the array is correlated with the rotations of individual paticles. By "global behavior" we mean the relation between the force applied $N_L - N_0$ (Fig. 2) and the linear acceleration $\dot{v}$. The corresponding equation for a single block on the plane is simply Newton's law of motion supplemented by the friction law.

In the case of an array of particles, we have to consider equations of dynamics for individual particles. A friction law at interparticle and particle-plane contacts has to be implemented as well. It is clear that the problem in all its details cannot be solved analytically. However, two considerations make an analytical study possible. First, the rotation modes are experimentally well defined. According to Fig. 5, three *pure* phases of rotation come one after another along the array without mixing. In this way, the study of rotations can be done separately for each pure phase. Second, relying on simulations of Ref. [7], for a given force applied, the array achieves rapidly a steady state where the accelerations of all particles are constant. However, during one individual slip, the applied force on the system changes in time. In our experiments, the duration of one slip is, on average, of the order of 0.01 s. On the other hand, simulations show that for a completely random distribution of angular velocities, an array of ten particles of the same characteristics as in experiments takes not more than 0.01 s to achieve steady state. That is the reason why we expect that the slip period in our experiments is long enough to let the system follow very closely the steady-state path, at least at the beginning of a slip where the linear velocity of the array is not too high. In this way, all the analytical work can be concentrated only on the situation where the accelerations of the particles stay constant in time for a fixed value of the applied force. This will enable us to use directly the solution with steady accelerations and to ignore the transient regime.

A. Steady state

In the following, the masses of the particles, as well as their radii, are assumed to be unity. The acceleration of gravity has been set to unity as well. Then all quantities are dimensionless and the moment of inertia I is a mere geometric constant. The linear and angular velocities of the particle are, respectively, v and ω. All particles here are assumed to be rigid and thus they cannot interpenetrate.

With the conventions of Fig. 2, the equations of motion for each particle i are written

$$\begin{aligned} T(i) - T(i-1) + R(i) &= 1 \ , \\ N(i) - N(i-1) + S(i) &= \dot{v} \ , \\ T(i) + T(i-1) - S(i) &= I\dot{\omega}(i) \ . \end{aligned} \tag{3}$$

The boundary conditions are

$$N(L) = N_L \ , \quad N(0) = N_0 \ . \tag{4}$$

There are $5L + 1$ variables to be determined, whereas we have only $3L$ equations given by dynamics. The remaining $2L + 1$ equations are prescribed by the friction law at the $2L + 1$ contact points. For the purpose of the present study, we will consider the simple Coulomb law of friction with one coefficient of friction μ for the interparticle contacts and another coefficient of friction μ' for the plane-particle contacts [11,7]. We begin with the case of rolling on the plane (phase 1) and will show that this mode is naturally followed by the two other modes observed in experiments.

Since all of the particles in phase 1 are rolling in the same direction, friction forces at interparticle contacts are fully mobilized so that the equations of dynamics can

be supplemented in this case by

$$T(i) = -\mu N(i) \ , \quad \dot{\omega}(i) = \dot{v} \ . \tag{5}$$

From Eqs. (3) and (5) we get the expression for the friction force at particle-plane contacts

$$S(i) = \dot{v} - \frac{2\mu}{1+\mu}\left(N_0 + \frac{1+I}{2\mu}\dot{v}\right)\left(\frac{1+\mu}{1-\mu}\right)^i \tag{6}$$

and the limit on its value

$$|S(i)| \leq \frac{\mu'(1+\mu\dot{v})}{1+\mu\mu'} \ . \tag{7}$$

Equation 6 shows that the particle-plane friction is mobilized progressively along the array and its direction depends on the linear acceleration of the array. The absolute value of the friction force has an upper bound given by Eq. (7). From Eq. (6) and (7)

$$i \leq L_1 = 1 + \left\{\ln\left(\frac{1}{2\mu}\frac{1-\mu}{1-\mu\mu'}(\dot{v}+\mu')\right) - \ln\left(N_0 + \frac{1+I}{2\mu}\dot{v}\right)\right\} \Big/ \ln\left(\frac{1+\mu}{1-\mu}\right) \ , \tag{8}$$

where L_1 is the length of phase 1. The contacts of the particles following the particle $i = L_1$ can no longer be nonsliding on the plane. In phase 2, all contacts are sliding while the particles continue rotating in the same direction.

Let us consider the situation where all contacts are sliding with all particles rotating in the positive direction (phase 2). The following equations are then to be supplemented to the equations of dynamics:

$$\begin{aligned} T(j) &= -\mu N(j) \ , \\ S(j) &= -\mu' R(j) \ , \\ \dot{\omega}(j) &> 0 \ . \end{aligned} \tag{9}$$

From these equations and those of dynamics we get the expression for the angular accelerations

$$I\dot{\omega}(j) = -\frac{2\mu(\mu'+\dot{v})}{1-\mu\mu'}j + \frac{\mu(1+\mu')}{1-\mu\mu'}\dot{v} + \frac{\mu'(1+\mu)}{1-\mu\mu'} - 2\mu' N(j=0) \ , \tag{10}$$

where j designs the jth particle of phase 2 and $N(j=0)$ is the normal interparticle force on the first particle in the phase. At the same time

$$S(j) = -\frac{\mu'(1+\mu\dot{v})}{1-\mu\mu'} \ . \tag{11}$$

These equations show that the angular acceleration is decreasing linearly with the particle number while the friction force at particle-plane contact remains constant. However, positivity of the angular acceleration, as the consistency condition, gives the maximum number of particles in the phase

$$j \leq L_2 = \frac{1}{\mu'+\dot{v}}\left[\frac{1+\mu'}{2}\dot{v} + \frac{\mu'(1+\mu)}{2\mu} - (1-\mu\mu')N(j=0)\right] \ , \tag{12}$$

where L_2 is the length of phase 2. From the end of phase 2, the particles can no longer keep rotating consistently in the same direction.

Let us now consider phase 3, where the interparticle contacts can no longer be sliding. The equations to be supplemented to the equations of the dynamics are

$$S(k) = -\mu' R(k), \quad \dot{\omega}(k) = -\dot{\omega}(k+1) = \dot{\omega} \ , \tag{13}$$

where k is the kth particle in the phase. Assuming that the first particle in this phase in contact with the last particle of phase 2 has a negative rotation velocity, we get immediately the expression for the tangential interparticle force

$$T(k) = \left[T(k=0) + \frac{\mu'}{2} + \frac{I\dot{\omega}}{2\mu'}\right]\left(-\frac{1+\mu'}{1-\mu'}\right)^k - (-1)^k\frac{I\dot{\omega}}{2\mu'} - \frac{\mu'}{2} \ . \tag{14}$$

The interparticle friction oscillates with a period of two particles and grows exponentially. We remark that this behavior of the interparticle friction force is only related to the fact that the interparticle contacts here are nonsliding. Even in the case when $\dot{\omega} = 0$, which is a particular case of phase 3, this oscillating behavior is obtained. In the same way, we get the expression for the normal interparticle force

$$N(k) = N(k=0) + k(\dot{v}+\mu') + \mu'\left[T(k=0) + \frac{\mu'}{2} + \frac{I\dot{\omega}}{2\mu'}\right]\left[1 - \left(-\frac{1+\mu'}{1-\mu'}\right)^k\right] \ . \tag{15}$$

From Eqs. (14) and (15) and the boundary condition $T(0) = -\mu N(0)$, it is easy to see that $|T(k)| \leq \mu N(k)$ for all k. Thus the length of phase 3 is not limited by the mobilization of interparticle friction forces. However, some limit arises from the normal particle-plane force, which, for the sake of consistency of the equations, has to be positive. The expression of the normal particle-plane force is

$$R(k) = 1 + (-1)^k\frac{I\dot{\omega}}{\mu'} + \frac{2}{1-\mu'} \times \left[T(k=0) + \frac{\mu'}{2} + \frac{I\dot{\omega}}{2\mu'}\right]\left[-\frac{1+\mu'}{1-\mu'}\right]^{k-1} \ . \tag{16}$$

The positivity of $R(k)$ sets an upper limit on the length of phase 3:

$$k \leq L_3 = 1 + \left\{\ln\left[\frac{1-\mu'}{2}\left(1 + \frac{I\dot{\omega}}{\mu'}\right)\right] - \ln\left[T(k=0) + \frac{\mu'}{2} + \frac{I\dot{\omega}}{2\mu'}\right]\right\} \Big/ \ln\left(\frac{1+\mu'}{1-\mu'}\right), \tag{17}$$

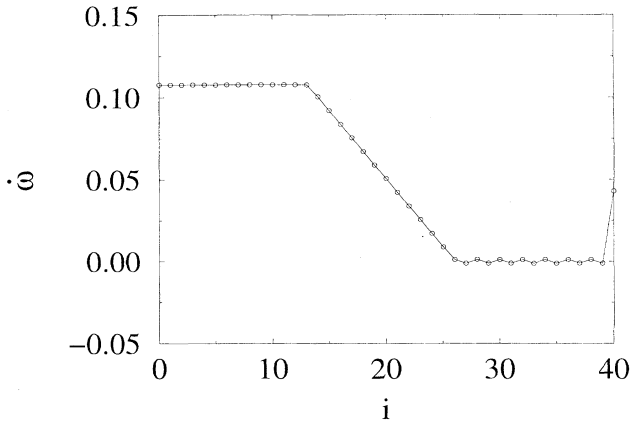

FIG. 10. Angular acceleration as a function of the particle position in an array of 40 particles in the steady state, where all the accelerations remain constant in time. All accelerations are normalized with respect to the constant of gravity. The acceleration on coordinate 0 stands for the translational acceleration. The coefficients of interparticle and particle-plane friction are 0.01 and 0.1, respectively. The driving force and the confining force are 8.0 and 0 times the weight of one particle, respectively.

where L_3 is the maximum length of the phase. The particle just behind the particle $L_1 + L_2 + L_3$ will rise up as the reaction force on the plane vanishes. Hence, for the array to be stable (no contact opening), we should have $L \leq L_1 + L_2 + L_3$.

These features of rotation modes in the steady-state regime are very close to those observed in our experiments. The three phases along the array appear naturally from a progressive mobilization of friction forces at nonsliding contacts and the consistency of rotation modes. The expressions of the lengths of phases contain the linear acceleration of the array $\dot{v}$ or the angular acceleration of particles $\dot{\omega}$ in phase 3. The relation between

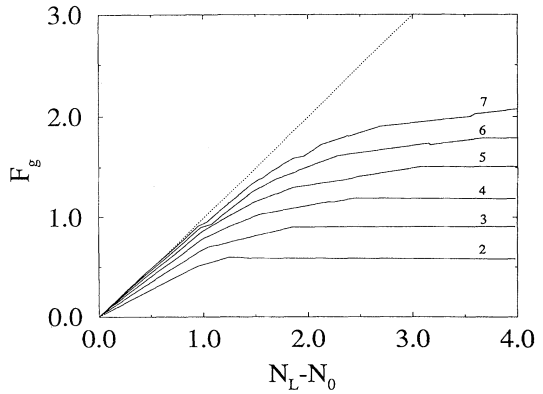

FIG. 11. Global friction force F_g on the plane as a function of the applied force $N_L - N_0$ for arrays composed of different numbers of particles in the steady state. The parameters are $\mu = 0.3$, $\mu' = 0.3$, and $N_0 = 0.01$. Simulations have been done with the exact Coulomb law of friction. All forces are normalized with respect to the weight of one particle.

$\dot{v}$ and $\dot{\omega}$ in phase 3 is to be looked for in the boundary conditions. It can be shown that $\dot{\omega}$ in phase 3 decreases with the coefficient of friction between the last particle and the pushing block.

Figure 10 shows the angular acceleration as a function of the particle position in an array of 40 particles, as obtained from a direct simulation [7]. The three rotation modes appear clearly on this figure. The lengths of these modes are in excellent agreement with the analytical expressions derived above on the basis of the experimental observation that the first particle is in mode 1. The rotation of the last particle depends directly on the coefficient of friction between this particle and the pushing block. In the same way, Fig. 11 shows the total friction force F_g on the plane as a function of the applied force for arrays of different sizes as obtained in simulations. The global friction increases with the applied force on the array to saturate finally to a value equal to the particle-plane coefficient of friction times the total weight of the array. These curves show three different regimes: two quasilinear regimes for small and large values of the applied force and a transition between these two asymptotic regimes. These regimes are dominated, respectively, by phases 1, 3, and 2.

B. Stick-slip motion

The foregoing analysis of the steady-state motion holds for a given applied force on the array. In the following we will introduce a simple argument based on the force diagrams of Fig. 11 in order to account for the evolution of the system during one slip and the expected experimental consequences.

Let us first recall briefly the dynamics of a solid block (with no rotational degrees of freedom) pulled by a spring moving at constant speed v on a horizontal plane. Let k be the spring constant and x the position of the block on the plane. Let $\epsilon = vt - x$ be the elongation of the spring. When the spring is pulled, the body first stays at rest (stick phase). Since the friction force is mobilized at the contact with the plane to compensate exactly the spring tension, $N = k\epsilon$. This stick phase is possible up to the maximum value $F = mg\mu_s$ of the friction force, where μ_s is the static coefficient of friction. The block starts to slip, opposing the motion by a dynamic friction force $mg\mu_d$ [10]. In the simplest approximation, μ_d is constant and does not depend on the velocity of the block. The motion is at first accelerated and then decelerated, until $\dot{x} = 0$. The block sticks again to the plane and the friction force increases continuously due to constant pulling speed. The path followed by the system in the force space consists of a "slip path" and a "stick path." The stick path, where the friction force is equal to and opposite the applied force, is the line $N = F$. The slip path is the straight line $F = F_d$. There are two jumps in the friction force at the two transition points between the two paths. The intersection point between the stick path and the slip path is the center of oscillations. This is a stable fixed point if the slope of the slip path is smaller than that of the stick path. This is the most basic image of the dynamics of stick-slip motion since the dynamic

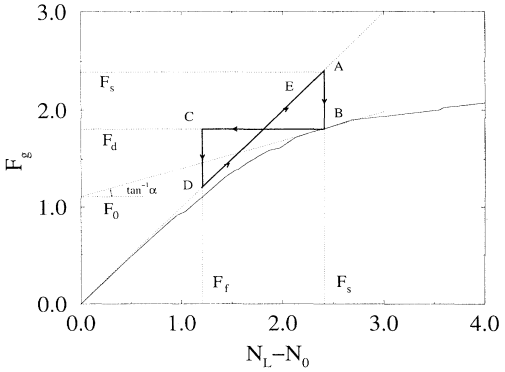

FIG. 12. Global friction force F_g on the plane as a function of the applied force for an array of 7 particles with the same parameters as in Fig. 11. A possible stick-slip path $ABCDE$ is shown. All forces are normalized with respect to the weight of one particle.

coefficient of friction is independent of velocity and the transitions take place in a discontinuous manner. The equation of motion is written

$$\begin{aligned} &m\ddot{\epsilon} + k\epsilon = mg\mu_d \quad \text{if } \dot{x} \neq 0 \ , \\ &\ddot{\epsilon} = 0, \ F = N = k\,\epsilon \ \text{ if } \dot{x} = 0 \ . \end{aligned} \tag{18}$$

The orbit of this motion in the phase space $(\epsilon, \dot{\epsilon})$ is a semicircle for the slip path and the straight line $\dot{\epsilon} = 0$ for the stick path. The center of oscillation in the force space is given by $F_d = k\epsilon_d = mg\mu_d$. Equation (18) is symmetric with respect to ϵ_d, so that the force drop ΔF is related to the coefficients of friction by

$$\Delta F = 2\,(F_s - F_d) = 2\,mg(\mu_s - \mu_d) \ . \tag{19}$$

Note that fluctuations of μ_s would induce random values of the force drop, which plotted against the slip force would define a straight line of slope 2. Hence the slope 2 is a signature of the symmetry of motion around the center of oscillations. As detailed in Sec. II, our experiments with the Plexiglas-polystyrene system give a slope of 1.6 for the $F_s - \Delta F$ diagram, thus showing the dissymmetric behavior of the stick-slip oscillations of an array of particles.

A simple representation of the stick-slip motion of an array of particles in the force space is obtained if we assume that the steady-state diagram of the global friction as a function of the driving force (Fig. 11) controls the effective slip path of the array. Figure 12 shows the theoretical $F_s - \Delta F$ diagram for seven particles and a possible slip path. A slip is initiated as soon as the global friction force F_g reaches a static threshold on the stick path $N_L - N_0 = F_g$ (point A on the figure). The friction force is rapidly reduced to the corresponding dynamic friction force on the diagram (point B). If the array exactly followed the steady-state path, it would go very close to the origin on the steady-state diagram and thus the coefficient of dynamic friction would be very small. This is in contrast with our experimental observations and suggests that, as the linear velocity of the array increases, the global friction F_g does not decrease as rapidly as on the steady-state diagram. A simple approximation is to assume that F_g remains constant (the path BC). When the velocity of the array becomes zero, the global friction is reduced to the corresponding static value on the stick path (point D). The stick path is then followed by the array up to a new static threshold (point E on the figure).

The main difference between this simple model for the array of particles and the stick-slip motion of a block is that the initial point of the slip path (B) for an array of particles is on the steady-state path, which is not constant as a function of the applied force $N_L - N_0$. Let α be the mean slope of the steady-state path in the transition regime between the two asymptotic regimes. Experimentally, this regime is the most active region in the force space since not all particles are in rolling phase. As the initial point of the slip path is on the steady-state path, we have

$$F_d = \alpha F_s + F_0 \ . \tag{20}$$

On the other hand, the force drop ΔF_g is given by

$$\Delta F_g = F_s - F_f = 2(F_s - F_d) \ . \tag{21}$$

From Eqs. (20) and (21) we get the relation between the slip force and the force drop

$$S_s = \frac{\Delta F_g}{F_s - \frac{F_0}{1-\alpha}} = 2(1-\alpha) \ . \tag{22}$$

This equation shows that the force drop varies linearly with the static threshold and the slope is $2(1-\alpha)$, which is smaller than 2. This equation for the Plexiglas-polystyrene system, with a slope of $S_s = 1.6$, yields the value $\alpha = 0.2$, which is in good agreement with the theoretical slope in Fig. 12. We have seen (Fig. 9) that the force drop for five and six particles is relatively high. Figure 11 shows that the details of the steady-state paths are rather complicated and it is not straightforward to relate them to the experimental observations. However, a qualitative change is observed on Fig. 9 near the stick path in transition from five to six particles.

Our theoretical approach does not take into account the static coefficient friction at the particle level. So the global static threshold of the array remains undefined. The introduction of static friction at the particle level has an important theoretical consequence, namely, the multiplicity of solutions even when the system is in motion and obviously a multiplicity of solutions at static equilibrium. Such a system with multiple coefficients of friction in statics and in dynamics can develop, following the same lines of reasoning presented in this section: irregular stick-slip oscillations like those observed in experiments. Fluctuations of the static threshold have a direct consequence on the rotations modes of the array. In our experiments the first two or three particles are always in phase 1. Depending on the position of the initial point of the slip path, there is a varying number of particles in phase 1. Moreover, some particles initially in phase 2 or 3 may enter phase 1 as the driving force decreases. Hence the total rotation of each particle during

an experimental run is the sum of two contributions: a regular part related essentially to its position in the array, as described in Sec. III A, and an additional rotation due to the transient in rolling mode because of fluctuations of the static threshold or variation of the applied force. The additional rotation is proportional to the total time a particle is in rolling phase. Now it is clear that, as the driving force decreases, a particle with a smaller label (Fig. 2) enters the rolling mode before a particle with a greater label. This fact explains the rotation modes observed in Fig. 5(b). This mode is observed only with the Plexiglas-polystyrene system whose dynamic coefficient of friction is relatively low with respect to its static coefficient of friction. The result is large force drops and a long excursion on the slip path. The velocity gradient superposed on the three phases should result from this excursion and the onset of the rolling mode of successive particles in the rolling mode. In other cases, with smaller force drops, we observed only regular rotation modes like in Fig. 5(a), which are well explained by a steady-state approach (Sec. III A).

We consider the present study as a first approximation approach to the problem of stick-slip dynamics of a granular system. The complexity of the problem results from the lateral contacts between the particles. "Irregular" stick-slip motions are observed also in dry friction of a single block for some ranges of values of parameters such as the driving speed and the stiffness of the pushing device [9]. The present study suggests that such behaviors may well result from the bulk properties of the material (elasticity, etc.) or the experimental setup.

IV. CONCLUSION

We have investigated frictional properties of an array of particles in stick-slip oscillation. The behavior of this system is surprisingly rich in contrast with its apparent simplicity. Well-defined rotation modes are developed along the array, with characteristic lengths intermediate between the particle size and the system size. These intermediate length scales appear as a result of the interplay of the friction law and the dynamics and suggest that the transition from a discrete to a continuous description has to be mediated by mesoscopic length scales.

Our experiments show that an array of particles behaves essentially like a single block with mean global static and dynamic coefficients of friction. However, these coefficients of friction both increase with the number of paticles. Moreover, the motion is not quite symmetric around the center of oscillations. A simple model based on the steady-state force diagram of the array accounts for this dissymmetry.

Let us finally emphasize the sensitivity of this system to noise, well quantified in this model. The global friction force on the plane is a rapidly increasing function of a small confining charge. More generally, the coherent motion of particles observed in rotation modes suggests that the dynamics cannot smooth out noise as is the case in thermodynamic systems. The noise is rather taken into account by the dynamics. In this respect, stick-slip dynamics against a rigid boundary shows the same features as avalanche dynamics at the free surface of a sandpile: regular behavior of the mean values and macroscopic fluctuations around mean values. Although a steady-state approach seems to explain many features of the experimental observations, extensions of the theoretical model to incorporate static coefficient of friction are presently under study.

ACKNOWLEDGMENTS

We would like to thank J. P. Troadec for many useful discussions. M. Ammi and T. Le-Pennec are acknowledged for their kind help during the experiments at Université de Rennes. This work was supported by the CNRS Groupement de Recherche "Physique des Milieux Hétérogènes Complexes" and GEO. This investigation is presently a subject of collaboration with Hochstleistungsrechenzentrum Supercomputing Center in Jülich-Germany.

[1] P. Bak, C. Tang, and K. Wiesenfeld, Phys. Rev. Lett. **59**, (1987); Phys. Rev. A **38**, 364 (1988).
[2] H. M. Jaeger, C.-h. Liu, and S. R. Nagel, Phys. Rev. Lett. **62**, 40 (1989).
[3] P. Evesque and J. Rajchenbach, C. R. Acad. Sci. Ser. II (Paris) **307**, 223 (1988).
[4] J. M. Carlson and J. S. Langer, Phys. Rev. Lett. **62**, 2632 (1989); Phys. Rev. A **40**, 6470 (1989); M. de Sousa Vieira, G. Vasconselos, and S. R. Nagel, Phys. Rev. E **47**, R2221 (1993).
[5] J. Schmittbuhl, Thèse de doctorat, Université Paris 6, 1994 (unpublished).
[6] J. P. Bardet and Q. Huang, in *Powders and Grains 93*, edited by C. Thornton (Balkema, Rotterdam, 1993).
[7] F. Radjai and S. Roux, Phys. Rev. E **51**, 6177 (1995).
[8] H. M. Jaeger and S. R. Nagel, Science **255**, 1523 (1992).
[9] A. Johansen, P. Dimon, C. Ellegaard, J. S. Larsen, and H. H. Rugh, Phys. Rev. E **48**, 4779 (1993).
[10] F. Heslot, T. Baumberger, B. Perrin, B. Caroli, and C. Caroli, Phys. Rev. E **49**, 4973 (1994).
[11] M. Jean and J. J. Moreau, in *Contact Mechanics International Symposium*, edited by A. Curnier (University of Romandes Press, Lausanne, 1992), p. 31.